Cardiomyocytes from phorbol myristate acetate-activated mesenchymal stem cells restore electromechanical function in infarcted rat hearts

Heesang Song[a,1], Hye Jin Hwang[b,1], Woochul Chang[b,1,2], Byeong-Wook Song[b,c], Min-Ji Cha[b,c], Il-Kwon Kim[b,c], Soyeon Lim[b,3], Eun Ju Choi[b,c], Onju Ham[b,c], Chang Youn Lee[d], Jun-Hee Park[d], Se-Yeon Lee[b,c], Eunmi Choi[b,e], Chungkeun Lee[f], Myoungho Lee[f], Moon-Hyoung Lee[g], Sung-Hou Kim[d,h,4], Yangsoo Jang[b,c,e,g,4], and Ki-Chul Hwang[b,c,e,4]

[a]Research Institute of Science for Aging, Yonsei University, Seoul 120-752, Korea; [b]Cardiovascular Research Institute and [c]Brain Korea 21 Project for Medical Science, Yonsei University College of Medicine, Seoul 120-752, Korea; [d]Department of Integrated Omics for Biomedical Sciences, Graduate School, Yonsei University, Seoul 120-749, Korea; [e]Severance Biomedical Science Institute, Yonsei University College of Medicine, Seoul 120-752, Korea; [f]Department of Electrical and Electronic Engineering, Yonsei University, Seoul 120-749, Korea; [g]Cardiology Division, Yonsei University College of Medicine, Seoul 120-752, Korea; and [h]Department of Chemistry, University of California, Berkeley, CA 94702

Contributed by Sung-Hou Kim, October 26, 2010 (sent for review September 2, 2010)

Despite the safety and feasibility of mesenchymal stem cell (MSC) therapy, an optimal cell type has not yet emerged in terms of electromechanical integration in infarcted myocardium. We found that poor to moderate survival benefits of MSC-implanted rats were caused by incomplete electromechanical integration induced by tissue heterogeneity between myocytes and engrafted MSCs in the infarcted myocardium. Here, we report the development of cardiogenic cells from rat MSCs activated by phorbol myristate acetate, a PKC activator, that exhibited high expressions of cardiac-specific markers and Ca^{2+} homeostasis-related proteins and showed adrenergic receptor signaling by norepinephrine. Histological analysis showed high connexin 43 coupling, few inflammatory cells, and low fibrotic markers in myocardium implanted with these phorbol myristate acetate-activated MSCs. Infarct hearts implanted with these cells exhibited restoration of conduction velocity through decreased tissue heterogeneity and improved myocardial contractility. These findings have major implications for the development of better cell types for electromechanical integration of cell-based treatment for infarcted myocardium.

cell therapy | optical mapping | differentiation | heart infarction | arrhythmia

Although various cell types have been considered for stem cell therapy to treat ischemic hearts (1–4), questions regarding the prevention of postinfarct arrhythmias and survival benefits remain unresolved (5). Previously, we published studies focused on enhancing the survival of mesenchymal stem cells (MSCs) transplanted in the harsh pathologic conditions of an infarcted myocardium (6–8). However, we found that such MSC transplantation does not provide a proportional survival benefit compatible with significant improvement in cardiac contractile function. One possible explanation for this discrepancy is that the focal application of MSCs that have not differentiated into electrically functional cardiomyocytes creates fixed heterogeneity among host tissues in the engrafted region, possibly predisposing the heart to ventricular arrhythmia.

Because ventricular arrhythmia is a common and lethal complication after myocardial infarction (MI) as well as recurrent MIs or cardiac rupture (9, 10), the development of cell types that are able to overcome the arrhythmic and electrophysiological consequences after transplantation is essential. In fact, the incomplete electromechanical integration leading to the equivalent incidence of arrhythmias with nonengrafted infarcted animals has been reported with many cell types, including skeletal myoblasts, ES cells, and MSCs (11). It seems that the focal application of MSCs could create fixed heterogeneity that disturbs the myocardial contractility and conduction velocity (CV) (9).

Although cardiomyocytes seem to be the most obvious resource for complete electromechanical integration, the procurement of a sufficient amount of cells is not yet achievable. In addition, differentiation of naive MSCs into cardiomyocytes has been observed only in vivo at extremely low rates, and their aptitude for electromechanical coupling is controversial (12). A cell type capable of electromechanically synchronizing with the surrounding myocardium and maintaining long-term electromechanical stability needs to be developed for use in clinical settings for infarcted hearts.

In our search for small molecules that induce the stem cell fate to specific lineages, we screened 189 chemicals (135 inhibitors and 54 activators of protein kinases) and found several compounds that induced differentiation of rat MSCs to myocytes. One of these, phorbol myristate acetate (PMA), a PKC activator, up-regulates cardiogenic properties from MSCs. This chemically activated cardiogenic MSC (ccMSC) prevents sudden death after engraftment into infarcted rats by electromechanically synchronizing with the host myocardium.

Results

MSC Therapy Is Insufficient for Prevention of Sudden Death in Infarcted Animals. MSCs were isolated from mixed culture with hematopoietic cells based on their attachment to the culture plate and further purified by exclusion with magnetic beads targeting the hematopoietic marker CD34. Yield was 3×10^6 cells (95% purity) after 2 wk of culture. Consistent with a previous report, the cultured MSCs expressed CD71, CD90, CD105, CD106, and ICAM-1, but not the hematopoietic and macrophage markers, CD34 and CD14, respectively (7, 8).

In our previous attempts to increase the beneficial effects of MSC transplantation (6–8), we found that MSC implants were suboptimal for improving survival, although treatment did reduce the incidence of sudden death in a rat model (31.6% in 19 MSC-injected vs. 55.6% in 27 sham-injected rats; $P = 0.14$; Fig. 1A). To investigate the poor performance of the MSC implants, we evaluated the recovery of histophysiology in MSC-engrafted myocar-
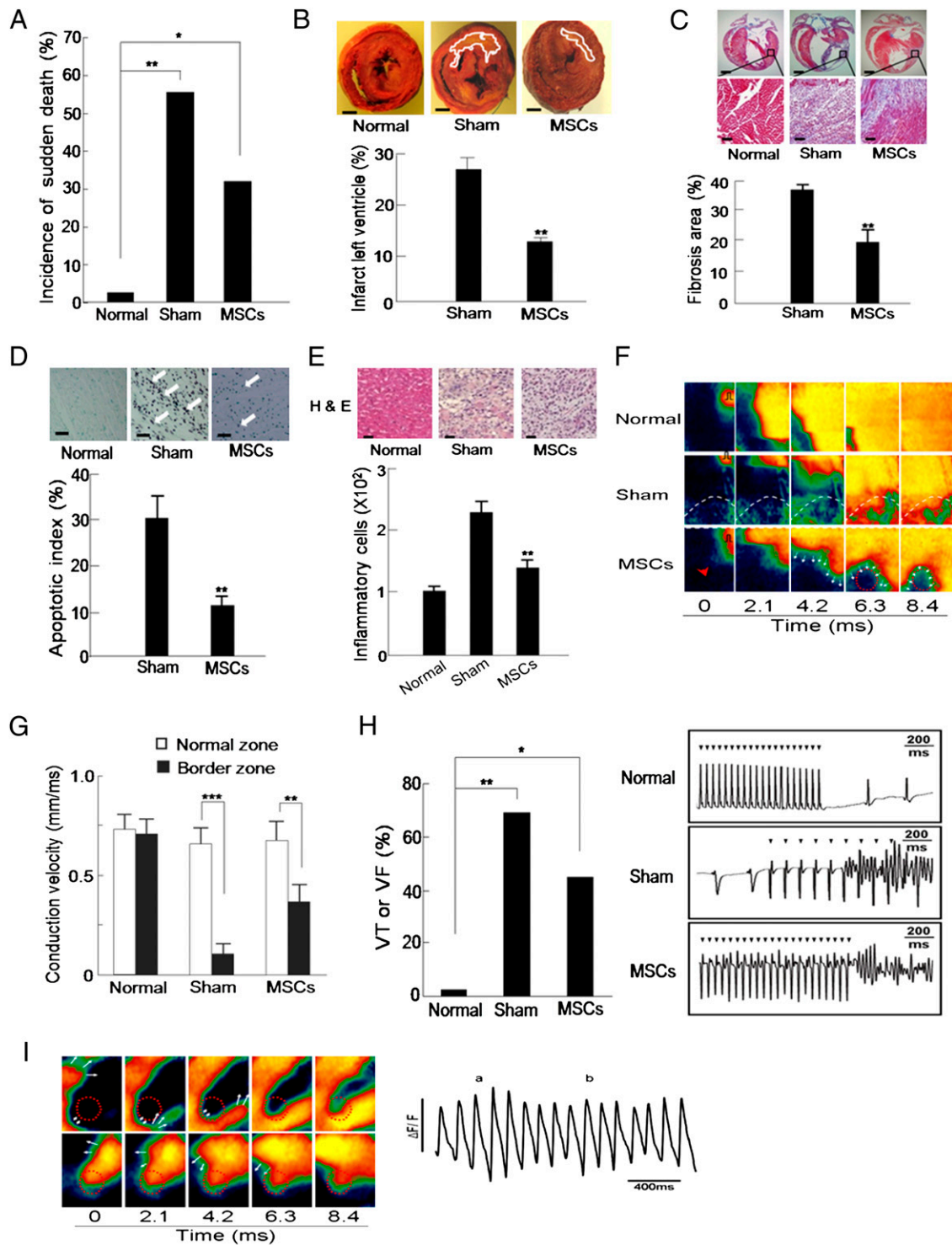
Fig. 1. Modest effects of MSC transplantation in infarcted myocardium. (*A*) Incidence of sudden death for normal (*n* = 12), sham-injected (*n* = 27), and MSC-transplanted (*n* = 19) rats during 11 d after transplantation. All rats that died during the procedure or immediately after cell implantation were excluded from the study (*SI Appendix, SI Methods*). (*B*) Triphenyltetrazolium chloride staining for determination of left ventricle infarct size. (Scale bar: 2 mm.) (*C*) Masson trichrome staining for determination of fibrosis area. (Magnification: 200×. Scale bars: *Upper*, 2 mm; *Lower*, 100 μm.) (*D*) TUNEL assay for the number of apoptotic cells. Representative site for TUNEL assay is the same as the Masson trichrome-stained region. Apoptotic nuclei are shown by white arrow. (Magnification: 200×. Scale bar: 100 μm). (*E*) H&E staining for identification of inflammatory cell infiltrates. (Magnification: 200×. Scale bar: 20 μm.) (*F*) Ectopic beats at border zone in normal and sham- and MSC-injected myocardium. (*G*) Local CVs were measured at the border zone in sham-treated (*n* = 8) and MSC-engrafted (*n* = 7) hearts. (*H*) VT or VF inducibility in normal (*n* = 12, *Top*), sham-treated (*n* = 13, *Middle*), or MSC-treated hearts (*n* = 9, *Bottom*). Arrows indicate electrical stimulation. (*I*) Sequential voltage map images during VT in the MSC-engrafted heart. Red circles and white arrows indicate the MSC-injected region and the direction of wavefront propagation, respectively. *Right*: Diagram shows an optical recording of the action potentials. All data are expressed as means ± SEM (*P < 0.05, **P < 0.01, ***P < 0.001).

MEDICAL SCIENCES

dium quantitatively. Although histological analysis showed that infarct size, fibrosis, and the number of apoptotic cells induced by ischemia were significantly decreased in the MSC-engrafted region compared with those in the sham-injected region (Fig. 1 *B–D*), these recoveries did not reach the level of the noninfarcted region and more than 50% of damages still remained in the region implanted with MSCs. In fact, remaining fibrosis may lead to continued electrical disturbances (5). We also observed that the MSC-injected group had fewer inflammatory cell infiltrates in the border region than did the sham controls (Fig. 1*E*). In addition, cardiac dimensions and systolic performances as measured by left ventricular catheterization were better in MSC-injected rats (*SI Appendix*, Figs. S1 and S2). Despite histological and functional improvements 7 and 11 d after transplantation, respectively, most of the engrafted MSCs did not express cardiac troponin T (cTnT),

suggesting that they were not yet differentiated into cardiomyocytes, whereby they might induce reentrant arrhythmia by acting as a current sink.

Alleviation of Electrical Vulnerability by MSCs Is Poor to Moderate.
We further evaluated the effect of MSCs on the electrical stability of the infarcted heart through optical mapping using Langendorff perfusion and an electrical vulnerability test in normal, sham-injected, and MSC-engrafted hearts 11 d after injury and treatment.

In MSC-engrafted hearts, action potentials displayed inhomogeneous and slow propagation into the infarct zone (Fig. 1*F*). Local CV from the activation time points of the action potentials was still depressed in the MSC-engrafted region compared with that of the noninfarcted region (Fig. 1*G*). In an
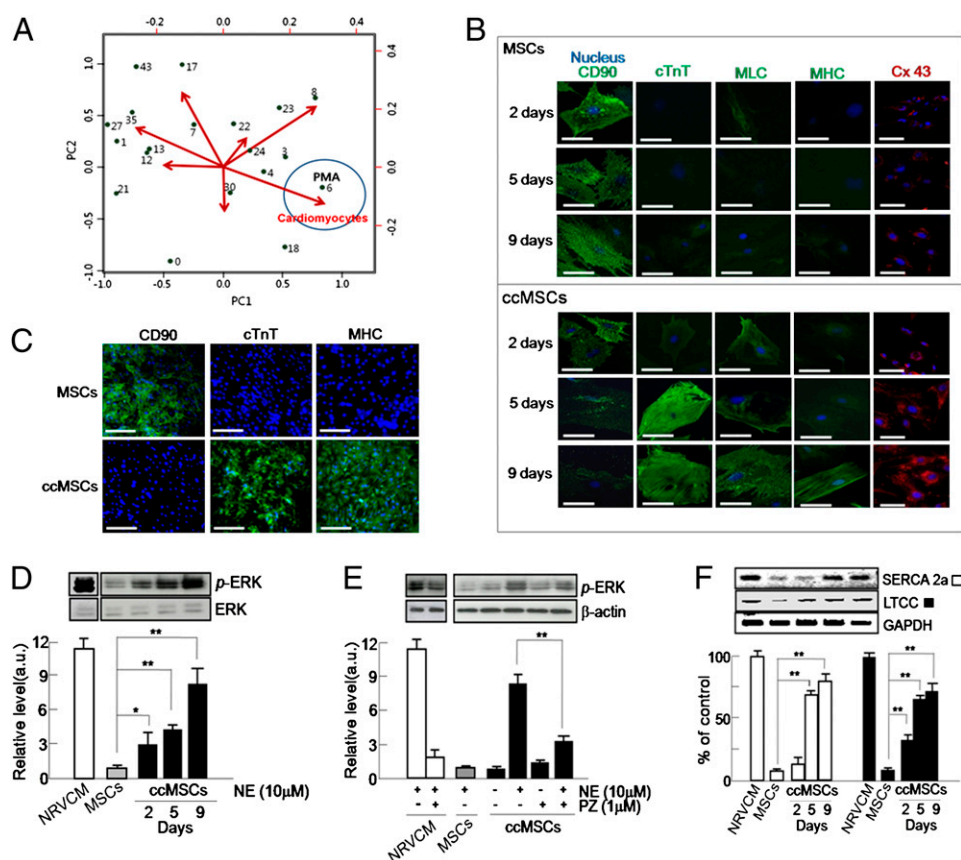

Fig. 2. Characterization of ccMSCs. (*A*) Principal component analysis (PCA) for small molecule-induced modification of MSCs. We obtained the coordinates of chemicals and target cell types by using the first two principal components from PCA and scaled the two sets of coordinates to plot them together in the map. The two largest principal components of PCA analysis are represented as PC1 and PC2. The spheres attached to the longer vectors are more efficient differentiation inducers for the cell types. The chemicals tested are indicated by green spheres (PMA is shown in blue) and the specific cell lineages are shown as red arrows. Tested molecules are from Calbiochem and are distinguished by numerals as follows: 0, no inhibitor; 1, 1,3-dihydro-1-(1-((4-(6-phenyl-1H-imidazo [4,5-g]quinoxalin-7-yl)phenyl)methyl)-4-piperidinyl)-2H-benzimidazol-2-one; 2, 1L6-hydroxymethyl-chiroinositol-2-(R)-2-O-methyl-3-O-octadecyl-sn-glycerocarbonate; 3, SH-5 ([(2R)-2-methoxy-3-octadecoxypropyl] (2,3,4-trihydroxy-6-methoxycyclohexyl) hydrogen phosphate); 4, lavendustin (5-(N-2′,5′-dihydroxybenzyl) aminosalicylic acid); 6, PMA (phorbol 12-myristate 13-acetate); 7, DMAT (2-dimethylamino-4,5,6,7-tetrabromo-1H-benzimidazole); 8, D4476 (4-(4-(2,3-dihydrobenzo[1,4]dioxin-6-yl)-5-pyridin-2-yl-1H-imidazol-2-yl)benzamide); 12, NU6102 [6-cyclohexylmethoxy-2-(4′-sulfamoylanilino)purine]; 13, [3-(pyridin-2-yl)-4-(4-quinonyl)]-1Hpyrazole; 17, H-89 [N-[2-((p-bromocinnamyl)amino)ethyl]-5-isoquinolinesulfonamide, 2HCl]; 18, SH-6 ([(2R)-2-methoxy-3-octadecoxypropyl] (2,3,4-trihydroxycyclohexyl) hydrogen phosphate); 21, Gö6983 (2-[1-(3-dimethylaminopropyl)-5-methoxyindol-3-yl]-3-(1H-indol-3-yl)) maleimide; 22, guanosine 3′,5′-cyclic monophosphorothioate, β-phenyl-1, N2-etheno-8-bromo-, Rp-isomer, sodium salt; 23, compound 56 (4-[(3-bromophenyl)amino]-6,7-diethoxyquinazoline); 24, SU11652 (5-[(Z)-(5-chloro-2-oxo-1,2-dihydro-3H-indol-3-ylidene)methyl]-N-[2-(diethylamino)ethyl]-2,4-dimethyl-1H-pyrrole-3-carboxamide; 27, N-(4-pyridyl)-N′-(2,4,6-trichlorophenyl) urea; 30, 4,5-dimethoxy-2-nitrobenzaldehyde; 35, SB 202190 [4-(4-fluorophenyl)-2-(4-hydroxyphenyl)-5-(4-pyridyl)1H-imidazole]; and 43, (5-PHENYL-2-ureido)thiophene-3-carboxamide. (*B*) Immunocytochemical determination for the altered expression of the MSC-specific marker CD90 and cardiac-specific markers cTnT, myosin light chain (MLC), myosin heavy chain (MHC), and Cx43 in control MSCs and the ccMSCs at the designated days after treatment. (Scale bar: 50 μm. Magnification: 400×.) (*C*) Immunocytochemical analysis for the homogenic characterization of the ccMSCs. Blue indicates nuclei and green is FITC for specific cardiac markers. (Magnification: 100×. Scale bar: 250 μm.) (*D*) Functional behavior of the ccMSCs by NE stimulus. (*E*) Blocking of NE-induced hypertrophic signals by prazosin. (*F*) Altered expression of Ca^{2+} homeostasis-related proteins sarcoplasmic reticulum Ca^{2+} ATPase (SERCA 2a) and L-type Ca^{2+} channel (LTCC) in MSCs and the ccMSCs. All data are expressed as means ± SEM (*$P < 0.05$, **$P < 0.01$).

Fig. 3. ccMSCs overcome postinfarct arrhythmia and mortality through electromechanical incorporation. (*A*) Immunohistochemical analysis between injected cells and the surrounded cardiomyocytes in the infarcted region. (Magnification: 200×. Scale bar: 100 μm.) (*B*) Representative examples of CV maps in MSC- and ccMSC-engrafted regions (white circle, 78 μm × 78 μm). (*C*) Real heart image and CV vector in MSC-engrafted (*Left*) and ccMSC-engrafted hearts (*Right*). Red boxes indicate cell-engrafted regions. Black boxes indicate optical view fields (10 mm × 10 mm). (*D*) Triphenyltetrazolium chloride staining for determination of left ventricle infarct size. (Scale bar: 2 mm.) (*F*) Masson trichrome staining for determination of fibrosis area (Magnification: 200×. Scale bars: *Upper*, 2 mm; *Lower*, 100 μm.) (*E*) TUNEL assay for the number of apoptotic cells. (Magnification: 200×. Scale bar: 100 μm.) (*G*) Immunostaining for fibrotic markers collagen I, fibronectin, and α-smooth muscle actin (α-SM actin). (Magnification: 200×. Scale bar: 50 μm.) (*H*) H&E staining for identification of inflammatory cell infiltrates. (Magnification: 200×. Scale bar: 20 μm.) (*I*) Surface ECG recording (lead II) from MSC- and ccMSC-engrafted rats. (*J*) Representative left ventricular pressure volume loops in ccMSC-engrafted rats. End-systolic pressure–volume relationship (ESPVR) during preload reduction is indicated by the dashed line. (*K*) Kaplan-Meier survival curves for normal (*n* = 12), sham-injected (*n* = 27), MSC-engrafted (*n* = 19), and ccMSC-engrafted rats (*n* = 12) 11 d after transplantation. All rats that died during the procedure or immediately after cell implantation were excluded from the study (*SI Appendix*, *SI Methods*). All data are expressed as means ± SEM (*$P < 0.05$, **$P < 0.01$).

electrical vulnerability test using the burst pacing protocol, ventricular tachycardia (VT) or ventricular fibrillation (VF) were induced in 69.2% of sham-operated rats ($n = 13$) and in 44.4% of the MSC-engrafted group ($n = 9$; $P = 0.38$; Fig. 1*H*), suggesting only moderate prevention of inducible reentrant ventricular arrhythmia by MSC transplantation. The MSC-engrafted site acts as an electroanatomical substrate for reentrant arrhythmia evoked by electrical stimulation (Fig. 1*I*). Therefore, modification of MSCs to cell types that are able to electromechanically synchronize with the surrounding myocardium before transplantation might be a better strategy for reducing tissue heterogeneity and to lower the incidence of VT.

PMA-Activated MSCs Exhibit Cardiogenic Properties. In a previous study, we showed that small chemical molecules, including protein kinase inhibitors, recognizably change stem cell fate (13). After screening 189 such small chemicals, we found that PMA, a PKC activator, specifically induced the expression of cardiogenic markers as revealed by sandwich ELISA (Fig. 2*A*). Immunocytochemical staining showed increased fluorescence of cardiac-specific markers such as cTnT, myosin light chain, and myosin heavy chain, but levels of the MSC-specific marker CD90 were lower after 9 d in the ccMSCs produced by PMA (Fig. 2*B*), which were consistent with the results of sandwich ELISA that the expression levels were significantly increased with time-dependent manner (*SI Appendix*, Fig. S3). In addition, we observed that the expression of the cardiac-specific transcription factor NkX2.5 was also significantly up-regulated in ccMSCs on sandwich ELISA (*SI Appendix*, Fig. S3). Interestingly, the fluorescence of connexin 43 (Cx43), a gap junction, was markedly increased in the ccMSCs (Fig. 2*B*). We observed that the cardiac phenotypes were similarly up-regulated in the ccMSCs (Fig. 2*C*), indicating that PMA endows MSCs with more homogeneous cardiogenic properties. In addition, the expressions of adrenergic and muscarinic receptors, which play critical roles in modulating cardiac functions such as heart rate and myocardial contractility (14–16), were significantly up-regulated in the ccMSCs compared with naive MSCs, except for α_{1D}, which is consistent with other results (17) (*SI Appendix*, Fig. S4 *A* and *C*). We further observed that phosphorylated ERK1/2 levels were significantly increased by norepinephrine (NE) in a time-dependent manner in both the ccMSCs and cardiomyocytes, but not in control MSCs that were blocked by prazosin, an α-adrenoreceptor blocker (Fig. 2 *D* and *E*), indicating that the ccMSCs are functionally active cells like cardiomyocytes. The expressions of sarcoplasmic reticulum Ca^{2+} ATPase and L-type Ca^{2+} channel, which are closely related to excitation–contraction coupling operated by Ca^{2+} influx in cardiomyocytes (18), were also significantly increased in the ccMSCs, but not in control MSCs, in a time-dependent manner (Fig. 2*F*). Collectively, these findings suggest that the ccMSCs are involved in the differentiating stage into cardiomyocytes or mature cardiomyocytes. This observation suggests that the activation by PMA triggers a cascade of transcriptional activation that regulates the differentiation of MSCs into cardiomyocytes.

ccMSC Engraftment Enhances Electrical Stability. We investigated the expression pattern of Cx43 in MSC- or ccMSC-engrafted regions because the incidence of VT is critically protected by the expression of Cx43 (19). We observed that Cx43 was expressed in a punctate fashion predominantly throughout the plasma membrane in the MSC-engrafted region, whereas Cx43 was detected mainly as plaques in the ccMSC-engrafted region, which indicated that the engrafted ccMSCs were well coupled with host cardiomyocytes through Cx43 (Fig. 3*A*). We further examined the electrical stability of cells in the ccMSC-engrafted hearts. On optical mapping, wave propagation during programmed electrical stimulation from the noninfarct site of the left ventricle base was markedly improved in the ccMSC-engrafted hearts. CV maps revealed marked restoration of CV in the ccMSC-engrafted region with recovery of local CV (0.71 ± 0.12 mm/ms; $n = 6$),

in contrast to partial restoration of CV in the MSC-engrafted region (0.38 ± 0.08 mm/ms; $n = 7$; Fig. 3*B*). The direction of the CV vector was homogeneous in the ccMSC-engrafted site compared with the MSC-engrafted site (Fig. 3*C*). In an electrical vulnerability test using a burst pacing protocol, VT induction was profoundly suppressed in the ccMSC-engrafted group [13% ($n = 8$) and 69.2% ($n = 13$) for ccMSC- and sham-injected groups, respectively].

ccMSC Engraftment Improves Cardiac Remodeling. As the restoration of CV and related arrhythmia protection results from additional paracrine effects of the ccMSCs on the surrounding tissue, we examined fibrosis, apoptosis, and inflammation in the engrafted region. Histological analysis showed that infarct size and interstitial fibrosis were markedly decreased in the ccMSC-injected rats compared with those in MSC-injected rats (Fig. 3 *D* and *E*). In addition, the number of apoptotic cells induced by ischemia in the transplanted region was significantly lower in the ccMSC-injected animals than in MSC-injected animals (Fig. 3*F*). The levels of immunostained collagen I and fibronectin decreased, whereas α-smooth muscle actin increased in the ccMSC-injected region compared with the MSC-injected region (Fig. 3*G*). We also observed that the ccMSC-engrafted region had fewer inflammatory cell infiltrates than did the MSC region (Fig. 3*H*). Moreover, we observed that the levels of proinflammatory cytokines such as IFN-γ, IL-1a, IL-1b, IL-6, and TNF-α that are increased by MI were significantly lower in the ccMSC-injected region than in the MSC-injected region (*SI Appendix*, Fig. S5 and Table S1). These results indicate that paracrine effects of the ccMSCs in injured myocardium could contribute to the elimination of tissue heterogeneity and, consequently, lead to CV restoration.

ccMSC Engraftment Prevents Sudden Deaths in Infarcted Rats. Surface six-lead ECG showed a shorter QRS duration in the ccMSC-engrafted rats compared with sham-injected and MSC-engrafted rats (Fig. 3*I* and *SI Appendix*, Table S2), indicating more homogeneous ventricular activation of the ccMSC-engrafted myocardium. In baseline surface ECG, premature ventricular contractions (PVCs) did not occur in the ccMSC-engrafted rats (0%; $n = 12$). To assess the electrical stability of the ccMSCs to catecholaminergic stimulation, we investigated the incidence of PVCs during systemic administration of isoproterenol. Catecholaminergic stimulation did not increase the occurrence of PVCs in the ccMSC-engrafted rats (*SI Appendix*, Fig. S6). The functional effects of the ccMSCs on infarcted hearts were evaluated by catheterization 21 d after injury and transplantation compared with those of MSC-engrafted hearts. Pressure-volume loop analyses showed less left ventricular dilation in the ccMSC-engrafted group compared with the MSC-engrafted group (Fig. 3*J*). The ccMSC transplantation resulted in a better catheterization-determined ejection fraction and a steeper slope of the end-systolic pressure–volume relationship, suggesting cardiac regeneration through the ccMSC engraftment (Fig. 3*J* and *SI Appendix*, Fig. S2). Ultimately, sudden deaths were markedly reduced in the ccMSC-transplanted rats in this study (Fig. 3*K*).

Discussion

MSCs offer several potential advantages over other types of stem cells for cardiac repair, but they still face several challenges that need to be addressed in preclinical studies, such as delivery, survival after transplantation, and electromechanical integration and safety (5). Although preconditioning of MSCs, including genetic modification, has increased their therapeutic potency (6–8, 20), the most obvious concern for clinical applications is how engrafted MSCs electromechanically integrate with host tissue (12).

In this report, we show that MSC-engrafted regions can function as electroanatomical substrates for the initiation of reentrant arrhythmia. However, remaining fibrosis in the MSC-engrafted region may lead to continued electrical disturbances, which is supported by reports that dense fibrosis presents a for-

midable physical barrier to cell regeneration (5) and acts as an electrical barrier that disturbs direct wave propagation, facilitating reentry (21, 22). Moreover, excessive inflammation in the MSC-engrafted region might also cause inhomogenous conduction and delayed repolarization (23, 24) as well as preventing the recruitment and survival of progenitor cells (25). Inexcitable properties of undifferentiated MSCs contribute to decreases in CV, increasing the susceptibility to ventricular arrhythmia and leading to sudden death. In fact, the results that action potentials displayed inhomogeneous and slow propagation into the infarct zone in MSC-engrafted hearts indicate that the conditions required to elicit stable reentrant circuit movement were not eliminated (26). The depressed local CV in the MSC-engrafted region may be attributable to the inexcitable nature of MSCs and their ability to act as a current sink (9, 12).

To create a cell type that is able to synchronize with surrounding cardiomyocytes electromechanically, we treated MSCs with PMA. This approach was inspired by the results from our previous study that small molecules, including protein kinase inhibitors, can change the fates of stem cells in recognizable ways (13). We found that PMA can induce the expression of cardiogenic markers. We showed that the transplantation of a unique cell type from MSCs exhibiting cardiogenic properties into the infarcted heart could help avoid problems caused by heterogeneity between the implanted cells and the myocardium, leading to further improvements in contractile function and electrical safety. Moreover, our result that Cx43 expression was markedly increased in the ccMSCs is supported by the result that Cx43-expressing cells prevent postinfarct arrhythmia (19). It is also reported that NE influences the contractile properties of the heart and induces a series of changes characteristic of the hypertrophic phenotype through α-adrenergic receptors in cardiomyocytes (14).

Nevertheless, it has to be further evaluated whether the implantation of ccMSCs may have additional beneficial effects that prevent other modes of sudden death, such as pump failure or asystole, because recent data showed that sudden death after acute MI in human patients may be a result of multiple different causes (10), even though arrhythmic death as a result of VT/VF is a possible cause of sudden death.

Ultimately, the application of this cell type may facilitate the prevention of sudden death caused by naive MSC transplantation, providing new strategies for enhancing electromechanical integration in cell-based therapy for MI. In addition, MSCs can be modified by PMA into cardiomyocytes that may better integrate with the electromechanisms of host tissue after engraftment, representing a promising therapeutic strategy for the clinical preparation of MSCs for transplantation to the infarcted myocardium.

We recognize that the differentiation of MSCs to cardiomyocytes involves elaborate orchestration of multiple signaling pathways and feedback circuits, and that PMA may, in vivo, modulate activities of molecules other than PKC. We present our results here because of their potential importance toward the development of clinically valuable cell types for cell therapy of MI. We plan to pursue more detailed studies on the molecular mechanisms of PMA and other chemicals that induce conversion of MSCs to ccMSCs.

Methods

Ex Vivo Modification of MSCs. At passage 2, MSCs were seeded in 60-mm plates at 2×10^5 cells/mL and treated with 1 μM PMA (Sigma) at a final concentration. The media were replaced with fresh PMA-containing media every 3 d for a maximum of 9 d.

Further detailed information on reagents and antibodies, cell culture, induction of MI and cell transplantation, histological analysis, optical mapping, catheterization, immunofluorescence, and other methods is given in *SI Appendix, SI Methods*.

1. Burt RK, et al. (2008) Clinical applications of blood-derived and marrow-derived stem cells for nonmalignant diseases. *JAMA* 299:925–936.
2. Vulliet PR, Greeley M, Halloran SM, MacDonald KA, Kittleson MD (2004) Intracoronary arterial injection of mesenchymal stromal cells and microinfarction in dogs. *Lancet* 363:783–784.
3. Perin EC, et al. (2003) Transendocardial, autologous bone marrow cell transplantation for severe, chronic ischemic heart failure. *Circulation* 107:2294–2302.
4. Wollert KC, et al. (2004) Intracoronary autologous bone-marrow cell transfer after myocardial infarction: the BOOST randomised controlled clinical trial. *Lancet* 364:141–148.
5. Segers VF, Lee RT (2008) Stem-cell therapy for cardiac disease. *Nature* 451:937–942.
6. Song H, et al. (2007) Tissue transglutaminase is essential for integrin-mediated survival of bone marrow-derived mesenchymal stem cells. *Stem Cells* 25:1431–1438.
7. Chang W, et al. (2009) Mesenchymal stem cells pretreated with delivered Hph-1-Hsp70 protein are protected from hypoxia-mediated cell death and rescue heart functions from myocardial injury. *Stem Cells* 27:2283–2292.
8. Song SW, et al. (2009) Integrin-linked kinase is required in hypoxic mesenchymal stem cells for strengthening cell adhesion to ischemic myocardium. *Stem Cells* 27:1358–1365.
9. Beeres SL, et al. (2007) Electrophysiological and arrhythmogenic effects of intramyocardial bone marrow cell injection in patients with chronic ischemic heart disease. *Heart Rhythm* 4:257–265.
10. Pouleur AC, et al.; VALIANT Investigators (2010) Pathogenesis of sudden unexpected death in a clinical trial of patients with myocardial infarction and left ventricular dysfunction, heart failure, or both. *Circulation* 122:597–602.
11. Laflamme MA, Murry CE (2005) Regenerating the heart. *Nat Biotechnol* 23:845–856.
12. Chang MG, et al. (2006) Proarrhythmic potential of mesenchymal stem cell transplantation revealed in an in vitro coculture model. *Circulation* 113:1832–1841.
13. Hwang KC, et al. (2008) Chemicals that modulate stem cell differentiation. *Proc Natl Acad Sci USA* 105:7467–7471.
14. Chien KR, Knowlton KU, Zhu H, Chien S (1991) Regulation of cardiac gene expression during myocardial growth and hypertrophy: molecular studies of an adaptive physiologic response. *FASEB J* 5:3037–3046.
15. Hosey MM (1992) Diversity of structure, signaling and regulation within the family of muscarinic cholinergic receptors. *FASEB J* 6:845–852.
16. Steinberg SF (1999) The molecular basis for distinct beta-adrenergic receptor subtype actions in cardiomyocytes. *Circ Res* 85:1101–1111.
17. Hakuno D, et al. (2002) Bone marrow-derived regenerated cardiomyocytes (CMG Cells) express functional adrenergic and muscarinic receptors. *Circulation* 105:380–386.
18. Shin SY, Choo SM, Woo SH, Cho KH (2008) Cardiac systems biology and parameter sensitivity analysis: Intracellular Ca2+ regulatory mechanisms in mouse ventricular myocytes. *Adv Biochem Eng Biotechnol* 110:25–45.
19. Roell W, et al. (2007) Engraftment of connexin 43-expressing cells prevents post-infarct arrhythmia. *Nature* 450:819–824.
20. Mangi AA, et al. (2003) Mesenchymal stem cells modified with Akt prevent remodeling and restore performance of infarcted hearts. *Nat Med* 9:1195–1201.
21. de Bakker JM, et al. (1993) Slow conduction in the infarcted human heart. 'Zigzag' course of activation. *Circulation* 88:915–926.
22. Anderson KP, et al. (1993) Myocardial electrical propagation in patients with idiopathic dilated cardiomyopathy. *J Clin Invest* 92:122–140.
23. Hoffman BF, Feinmark SJ, Guo SD (1997) Electrophysiologic effects of interactions between activated canine neutrophils and cardiac myocytes. *J Cardiovasc Electrophysiol* 8:679–687.
24. Ishii Y, et al. (2005) Inflammation of atrium after cardiac surgery is associated with inhomogeneity of atrial conduction and atrial fibrillation. *Circulation* 111:2881–2888.
25. Poss KD, Wilson LG, Keating MT (2002) Heart regeneration in zebrafish. *Science* 298:2188–2190.
26. Takahashi T, et al. (2004) Optical mapping of the functional reentrant circuit of ventricular tachycardia in acute myocardial infarction. *Heart Rhythm* 1:451–459.

MEDICAL SCIENCES